Microplastics exacerbate virus-mediated mortality in fish

Meredith Evans Seeley[1]†*, Robert C. Hale[1], Patty Zwollo[2], Wolfgang Vogelbein[1], Gaelan Verry[1], Andrew R. Wargo[1]

Affiliations:

[1]Virginia Institute of Marine Science, William & Mary, Gloucester Point, VA 23062

[2]William & Mary, Department of Biology, Williamsburg, VA 23187

*Correspondence to: meseeley@vims.edu

†Present affiliation: National Institute of Standards and Technology (NIST) and Hawaii Pacific University Center for Marine Debris Research, Waimanalo, HI 96825

Abstract: Microplastics are a persistent and increasing environmental hazard. They have been reported to interact with a variety of biotic and abiotic environmental stressors, but the ramifications of such interactions are largely unknown. We investigated virus-induced mortalities in a commercially important salmonid following exposure to microplastics, plastic microfibers, and natural (non-plastic) microparticles. Microplastics or microparticles alone were not lethal. Mortality increased significantly when fish were co-exposed to virus and microplastics, particularly microfibers, compared to virus alone. This presents the unique finding that microplastics (not natural microparticulate matter) may have a significant impact on population health when presented with another stressor. Further, we found that mortality correlated with host viral load, mild gill inflammation, immune responses, and transmission potential. We hypothesize that microplastics can compromise host tissues, allowing pathogens to bypass defenses. Further research regarding this mechanism and the interplay between microplastics and infectious disease are paramount, considering microplastics increasing environmental burden.

Keywords: microplastics, microfiber, virus, co-stressor, aquaculture, rainbow trout

30 **Graphical Abstract**

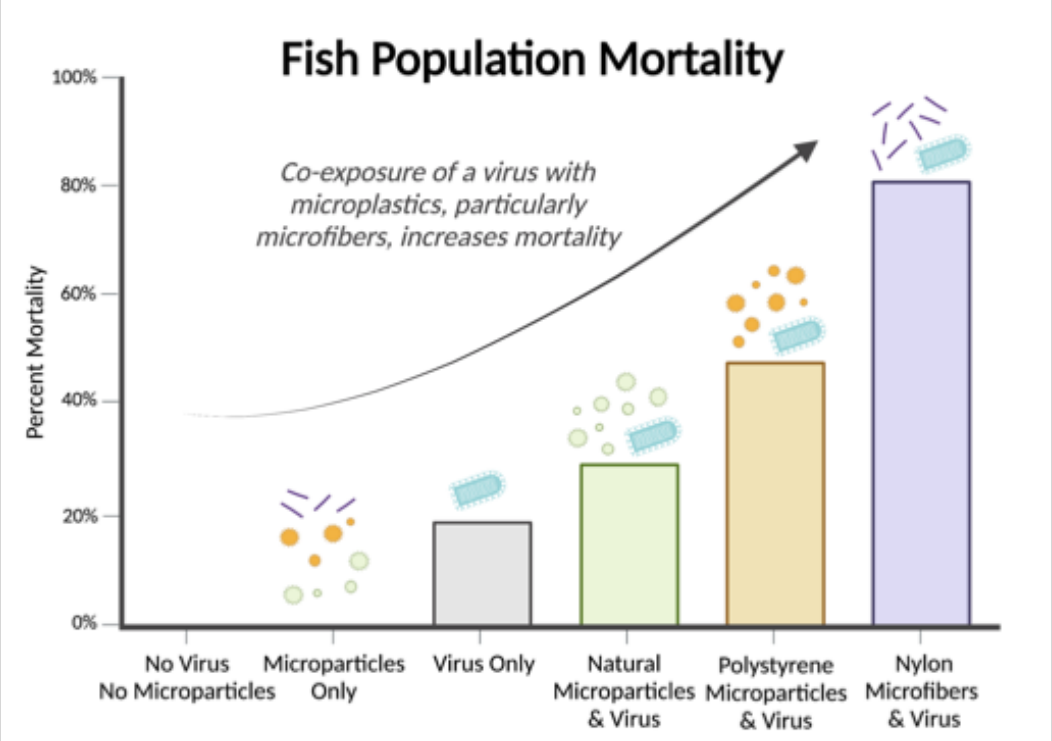

31

1. Introduction

Plastic production, use, and environmental release are increasing worldwide. Despite their longevity, plastics may weather and fragment into microplastics (≤ 5mm) over time. This has led to the ubiquitous accumulation of microplastics in aquatic, terrestrial, and atmospheric environments (Borrelle et al., 2020; Geyer et al., 2017; Hale et al., 2020). Humans are also exposed and microplastics have recently been detected in human blood and placenta (Leslie et al., 2022; Ragusa et al., 2021). While long presumed to be toxicologically inert, research suggests that plastic pollution presents health risks to living resources and humans (Bucci et al., 2020). Oversimplification of microplastics as a single homogeneous contaminant, however, ignores their toxicological complexity, as microplastics vary in size, shape, density, polymer chemistry, additive composition, and more (Rochman et al., 2019). Available research suggests that many effects of microplastics are sub-lethal and derive from their physical and chemical characteristics (Bucci et al., 2020; Zimmermann et al., 2019). Further, to date, the relative toxicities of naturally occurring polymeric microparticles (e.g., cellulose-based) have been rarely investigated despite their abundance in the environment. Thus, our ability to evaluate the toxicological significance of exposure to synthetic microplastics versus other microparticles is limited. Similarly, microfibers (as opposed to spheroidal microplastics) have been less commonly investigated despite their dominance in some environments (Athey and Erdle, 2021).

It has been postulated that microplastics may act in concert with other stressors, such as causative agents of infectious disease (pathogens) (Lamb et al., 2018; Leads et al., 2019; MacLeod et al., 2021). Indeed, pathogen fitness and virulence (i.e., infection-related morbidity and mortality) can be influenced by environmental pollutants (Springman et al., 2005). For example, prevalence of plastic debris and disease were reported to be correlated in Asian Pacific

55 corals (Lamb et al., 2018). Possible mechanisms include, but are not limited to: plastics act as a
56 sterile vector for pathogens (Amaral-Zettler et al., 2020); interactions of hosts with plastic causes
57 tissue damage and has deregulatory or pro-inflammatory effects on the immune system (Hale et
58 al., 2020; Zwollo et al., 2021); or coincident plastic, chemical (including contaminants sorbed to
59 the plastic surface), pathogen (e.g., arising from local human populations), and/or other
60 pollutant(s) combine to compromise the host. Available research is limited and has not yet
61 adequately clarified these interactions (Lamb et al., 2018; Leads et al., 2019). Considering the
62 ubiquity of microplastic pollution and pathogens in the environment, more research is warranted
63 to protect valuable resources. This is especially true for fisheries and aquaculture species, whose
64 environments can be both pathogen- and microplastic-laden (Jennings et al., 2016).
65 Here, we probed the effects of microplastics alone or with co-exposure to an aquatic virus
66 of worldwide concern, infectious hematopoietic necrosis virus (IHNV), on a species of
67 commercial and conservation relevance, rainbow trout (*Oncorhynchus mykiss*). This is a well-
68 studied virus and host, as IHNV leads to significant financial and ecosystem losses globally for
69 multiple types of salmonid species (Bootland and Leong, 2011; Dixon et al., 2016). We
70 evaluated resulting fish mortality and possible underlying histopathological and immunological
71 mechanisms. Microparticles included a polystyrene microplastic (expanded polystyrene, ground
72 and sieved to ~20 μm), nylon microfiber (10 x 500 μm flocking fibers), and a natural
73 microparticle, 'spartina' (marsh grass, *Spartina alterniflora*, washed, high-temperature dried,
74 ground, and sieved to ~20 μm). Microplastics were selected with consideration for the variety of
75 plastics that are used intensely in fisheries activities (e.g., polystyrene buoys and floats, nylon
76 nets or lines), as well as other sources. For example, polystyrene originating from building
77 insulation and single-use food containers is also commonly observed in stranded debris and

nylon fibers are widely used in textiles. Fish were exposed to microparticles in water at one of three concentrations over eight weeks. After four weeks, half of the fish were acutely exposed by immersion to a controlled dose of IHNV. For each treatment, fish were monitored for *in vivo* mortality and viral shedding. A fourth tank for each high particle concentration and controls (IHNV+ and -) was maintained for destructive sampling to analyze tissue viral load, histopathology, and immunological markers over time. We hypothesized that chronic exposure to polystyrene microplastics and nylon microfibers would increase IHNV virulence (compared to fish co-exposed to virus alone, or to the natural microparticle and virus), and that insights into the mechanism underlying virulence changes, as well as population level impacts, could be gained from viral load/shedding, histopathological and immunological analyses.

2. Methods

2.1 Particle Preparation

Expanded polystyrene foam, commonly used as building insulation, was purchased from a local houseware store. Foam was embrittled and ground in a Retsch CryoMill, sieved to ≤20 μm with Retsch AS 200 air jet sieve and Gilson Performer III Sieve shaker (Seeley et al., 2020). *Spartina alterniflora* (marsh cordgrass) was collected from estuarine marshes near Yorktown, VA by cutting dead stems near the base. Grass was sorted in a fume hood, washed with deionized water, and dried in a muffle oven at 60˚C. Sections were ground in a blender, then the Retsch CryoMill, and sieved as above. Undyed nylon 6’6 fibers were obtained from Claremont Flock, Inc. Fibers measured 0.8 denier (approximately 10 μm) in diameter and 0.5 mm in length. Size ranges of the particles were measured using a Beckman-Coulter Laser Diffraction Particle Size Analyzer, which measures the longest diameter of a particle. Photo-flo (© Eastman Kodak Company) was added to the particle/water mix to increase dispersion and decrease particle

clumping for analysis with the particle size analyzer (not in experiment). Particle size analysis confirmed the 500 x 10 µm measurement of nylon fibers provided by the manufacturer. The median diameter of polystyrene particles was 26.8 µm; 25% of particles were less than 16.4 µm. The median diameter of spartina particles was 39.2 µm; 25% of particles fell below 21.3 µm. Particle size analysis and microscopic images of particles are provided in Fig. S1. The data illustrated that spartina contained longer particles than polystyrene (a product of the plant cellular structure) which passed through the sieve via their shortest axis; this and any potential clumping may account for the overall greater size particles than polystyrene despite using the same sieving approach. The laser analyzed the nylon fibers at different orientations in the fluid. This likely accounts for the wide range of diameters measured. However, the predominance of measurements of 10 and 500 µm supported our expectation that these were the primary size axes of the nylon fibers (as provided by the manufacturer). The particles displayed similar behaviors and buoyancy in the experimental tanks, characterized by a brief period of floating on the water's surface (less than 10 minutes) and ultimately distributing within tank, a result of mixing from aeration.

2.2 Experimental Design and Procedures

Fertilized eyed rainbow trout (*Oncorhynchus mykiss*) eggs were obtained from the National Center for Cool and Cold Water Aquaculture in West Virginia (NCCCWA; within USDA's Agricultural Research Service). Trout were hatched and reared at the Virginia Institute of Marine Science (VIMS), according to guidelines from the Institutional Animal Care and Use Committee (IACUC-2020-06-24-14322-arwargo) and previously established protocols (Everson et al., 2021). Briefly, fish were maintained at 1-3% weight food, fed daily. Fish were initially

held in a specific pathogen-free recirculating system supplied with UV-irradiated fresh well-water at 12 ± 1˚C until reaching the desired size for experiments.

For the experiment, fish were transferred to a flow-through tower rack tank system (Aquaneering) housed in a BSL-II aquatic animal laboratory at VIMS, supplied by UV-irradiated fresh well-water at 15°C. Room air temperature was maintained at 15.8 ± 0.4˚C, water temperature at 15.0 ± 0.2˚C, dissolved oxygen at 100.1 ± 0.5% saturation, and lighting on a 12-hour diurnal cycle. Fish were housed in 6 L tanks (20 fish each) with one water line, two air stones, and fry screens, to facilitate particle circulation and oxygenation through the entire tank. Water flow rate was set to 300-350 mL min^{-1}. During the experiment, fish were fed 2.0% of their average body weight every four days, 1 hour after the start of a tank flush with fresh water (below). Average fish weight was 5.2 ± 0.4 g $fish^{-1}$ at the start of the experiment.

Fish received one of 20 possible treatments, outlined in Fig. 1 and Table S1. Each treatment contained triplicate tanks of 20 fish tracked for mortality and sampled for viral shedding. A fourth replicate was included for destructive tissue sampling in the high particle treatments and controls. Treatments and replicate tanks were randomly distributed throughout the tower rack system. For plastic exposure, fish were dosed with particles every other day, beginning on the first day of the experiment. In the first half of the experiment (weeks 1-4, prior to IHNV exposure) water in all tanks was held static for 24 hours during particle exposure. The flow was then resumed and tanks flushed for 24 hours to maintain water quality. Fish were switched to clean tanks after two weeks to remove buildup of feces debris and reduce ammonia levels (water ammonium maintained ≤5-8 ppm). In the second half of the experiment, the static plastic exposure period was reduced from 24 to ~10 hours, followed by a 38-hour flushing period rather than conducting tank changes to reduce risk of contamination of IHNV across tanks. In

total, the experiment lasted 56 days with 28 particle dosing events. Day 1 was considered the first day of fish exposure to microplastics. The experiment was monitored at the same time daily, recording temperature and dissolved oxygen continuously on YSI probes, and manually inspecting the number of fish mortalities in each tank.

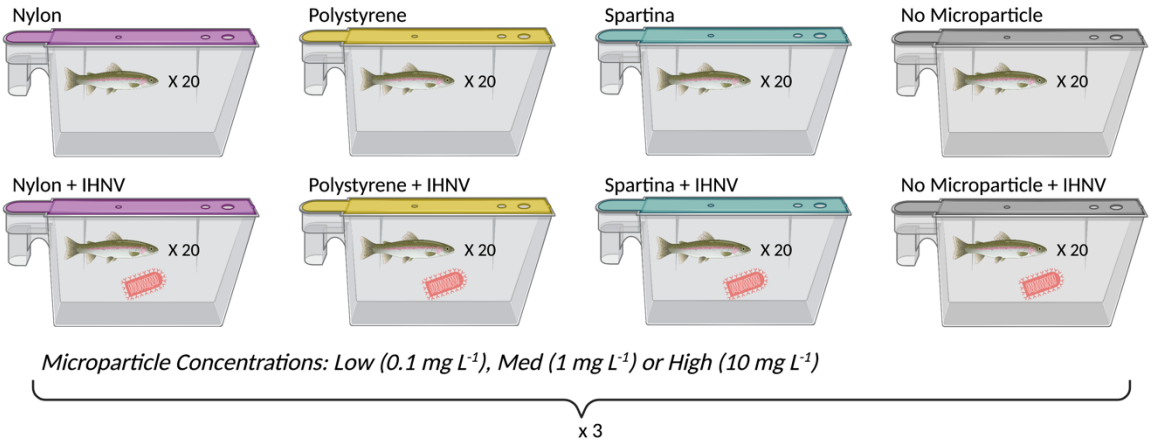

Fig. 1 Experimental design, consisting of 20 possible treatments. Fish were exposed to no microparticles or microparticles at one of three concentrations, in the presence or absence of virus. The high dose microparticle treatments and no particle treatments (IHNV+ and -) had a fourth replicate for destructive sampling, resulting in 68 tanks total (Table S1).

To reduce microplastic discharge to the local wastewater system, during the first hour of each tank flushing effluent was pumped through a series of in-line filters (75 µm, 20 µm, 5 µm and 1 µm), before passage through UV-irradiation (sufficient for virus inactivation) and eventual discharge to the municipal wastewater system.

Halfway through the experiment (day 28), fish were dosed with virus or a mock control. Experimental virus, IHNV (*Salmonid novirhabdovirus*) isolate C (genotype mG119M; GenBank accession number AF237984) was obtained from established laboratory stock (titer of 7.56×10^{8}

plaque forming units (PFU) mL^{-1}) diluted to 1.0×10^6 PFU mL^{-1} in Minimum Essential Media (MEM) with 10% fetal bovine serum (Jones et al., 2020). Fish were dosed with 5 mL of diluted IHNV stock in 995 mL water, to reach a final IHNV dose of 5.0×10^3 PFU mL^{-1}, in a 1-hr static immersion challenge, followed by resumption of water flow to the tanks(Jones et al., 2020). Non-virus (IHNV-) treatments were mock dosed with 5 mL of MEM with 10% fetal bovine serum.

To quantify viral shedding, 800 µL water samples were collected on days 28, 30, 32, 34, 36, 38, 40, 42, 48, and 54, from each of the triplicate survival analysis tanks per treatment. Water was collected at the end of the static period just prior to flushing, such that virus had maximum and consistent time to accumulate in tanks, then stored at -80˚C prior to extraction and analysis. A 210 µl volume of sampled water then underwent RNA extraction and quantitative real time polymerase chain reaction (qPCR) for IHNV quantification as detailed in Jones et al. 2020.

Tissue samples were collected following virus exposure on day 31, 35, 42 and 56 (3, 7, 14, and 28 days post-virus respectively; Fig. S2). Five fish were euthanized via overdose of tricaine methanesulfonate (MS-222) from each tissue sampling tank (Table S1) on each dissection day. On day 56 some tissue sampling tanks had less than 5 survivors, so fish were collected from survival analysis tanks of the same treatment, since it was the last day of the experiment and survival no longer needed to be tracked (number collected from another tank in no particle IHNV-: 3; no particle IHNV+: 3; spartina IHNV+: 2; polystyrene IHNV+: 4; nylon IHNV+: 5). Fish were weighed, and dissected following standard procedures to excise two gill arches (left side) and the anterior kidney (Gauthier et al., 2021). One gill arch and approximately 100 mg of anterior kidney tissues were preserved separately in 750 uL of RNAlater (ThermoFisher) for viral load and immune marker analysis and stored until RNA purification at -

185 80˚C. A second gill arch was preserved in a buffered formalin fixative (Z-Fix, Anatech) for
186 paraffin histology.
187 Routine methods of paraffin histology were used for the analysis of gill arches (Gauthier
188 et al., 2021). Briefly, individual gill arches were washed, decalcified, dehydrated in a graded
189 series of ethanols, cleared in xylene substitute, and embedded in paraffin wax. Tissue blocks
190 were sectioned to 5 μm with a rotary microtome, stained with haematoxylin and eosin, and
191 prepared slides were evaluated on an Olympus AX-70 photomicroscope, focusing analysis on the
192 best-preserved section of gill tissue for each sample. A severity scale 0-3 was applied for semi-
193 quantitative comparison between samples, where 0: no pathology observed, 1: mild (low-density
194 mild focal inflammation, no necrosis), 2: moderate (moderate density inflammation involving
195 ~10−25% area of tissue, moderate signs of early necrosis) and 3: severe (>25% area of tissue,
196 recruitment of immune cells, advanced necrotic region(s) and multiple areas of pyknosis,
197 karyolysis, and/or karyorrhexis).
198 Total RNA extraction from gill arches and anterior kidneys proceeded following Zwollo
199 et al., 2021. Briefly, RNA was purified using RNAzol RT (Sigma-Aldrich) reagent, which does
200 not require DNAse I treatment. Extracted RNA was quantified using a Nanodrop
201 spectrophotometer. RNA purity for all samples was ≥ 2.0 for 260/280, and as a secondary
202 measure, 230/280 ratios were ≥2.0.
203 cDNA was synthesized with iScript™ Reverse Transcriptase Supermix (Bio-Rad
204 Laboratories), using 1 ug of total RNA in a 20 uL reaction, according to manufacturer's
205 instructions. Quantitative real time polymerase chain reaction (qPCR) was used to quantify
206 number of copies of IHNV N-gene in parallel with analytical standards (Purcell et al., 2013), as
207 well as immune markers membrane-bound immunoglobulin mu (memHCmu), secreted

immunoglobulin mu (secHCmu), secreted immunoglobulin tau (secHCtau), interferon gamma (IFNγ) and macrophage colony-stimulating factor receptor (MCSFR). Reactions were run at 25 µL total volume containing 1 µL of cDNA, and using 60˚C annealing temperature. Primers and probe sequences and references can be found in Table S3. In general, five fish were included per treatment; in certain cases, a sample was removed due to poor RNA quality, detailed in Table S2. All TaqMan probe sequences (N-gene, secHCtau) were run in a single replicate per fish, while SybrGreen probe sequences were ran in triplicate per fish. IHNV N-gene was expressed as the log-adjusted viral RNA copy number per µg extracted RNA (Jones et al., 2020). For all immune markers, the relative fold change (RFC) was calculated using critical threshold (Ct) values, normalized to the no particle IHNV- control on day 31, according to Livak and Schmittgen, 2001 $2^{-\Delta Ct}$ method (Livak and Schmittgen, 2001), which does not require a reference gene. ARP gene expression was also quantified and explored as a reference gene control, but found to be differentially expressed through time, despite similar total RNA extraction yields. Differences in yield were accounted for by loading the same amount of RNA in RT reactions as discussed above. Tissues collected on day 56 (28 days post-IHNV exposure) were not analyzed for viral load or immune gene expression.

2.3 Statistical Analyses

All graphical and statistical analyses were completed in R and significance was inferred with $\alpha = 0.05$. For all data sets, every possible combination of fixed and random effects was modeled, and the best fit model determined using Akaike Information Criterion (AIC) and parsimony, with significance at Δ AIC ≥ 2 (R package 'stats' version 4.0.5) (RStudio Team, 2021). Statistical results are shown as test statistic value with factor and residual degrees of freedom given as subscripts.

231 Mortality analyses were visualized with Kaplan-Meier survival curves using package
232 'survival' (Fig.1) and differences between treatments determined with Cox proportional hazard
233 models in R with the "coxph" function (RStudio Team, 2021; Therneau, 2015). The maximum
234 model tested included fixed factors of virus presence/absence (2 levels: virus, mock; categorical),
235 a 'treatment' factor in which microparticle dose and type were combined (10 levels: no particle,
236 low nylon, medium nylon, high nylon, low polystyrene, medium polystyrene, high polystyrene,
237 low spartina, medium spartina, and high spartina; categorical) and their interactions, and random
238 factor of tank. A first analysis was conducted to investigate the effect of virus exposure on
239 survival, with only the factor virus and the other factors pooled. Because no mortality was
240 observed in IHNV- treatments, a second analysis was conducted among IHNV+ fish only, to
241 avoid issues related to non-proportional hazards (same fixed and random factors) and failed
242 convergence of interactions between treatment/virus. This model was used to report significant
243 differences between IHNV+ control (no particle) and all IHNV+ particle co-exposure treatments.
244 IHNV load in water was illustrated for all tanks treated with virus for high concentration
245 only (Fig. 3A) and all concentrations in the supplement (Fig. S3). Tanks not treated with virus
246 and day 28 (day 0 after virus exposure) were not included in statistical analyses, because
247 virtually no fish had started shedding virus by day 28 and our goal was to determine how viral
248 load differed after the point shedding began. Statistical analyses were conducted with a linear
249 fixed effects model (R package 'nlme' version 3.1-152) (Pinheiro et al., 2021). The maximum
250 model tested included fixed factors as above including treatment, day (continuous variable) and
251 their interactions, and the random factor of tank; with log10(Viral RNA copies/ug RNA) as a
252 response variable. The best fitting model included treatment, day, and their interaction, as well as
253 the random influence of tank.

IHN viral load (log10 transformed) in gill and anterior kidney samples were analyzed separately for each tissue type using a linear model (R package 'stats' version 4.0.5) (RStudio Team, 2021). The maximum model included categorical factors of microparticle, collection day, and their interactions. The best model for both anterior kidney and gill included the microparticle treatment and collection day; the model for anterior kidney included their interaction, while gill did not.

Gills pathological severity scale was illustrated including all fish sampled (n = 5), apart from four gills that were not successfully embedded for analysis (n = 4 for spartina IHNV- day 31, nylon IHNV- day 42, polystyrene IHNV+ day 56, no particle IHNV+ day 56 n = 4). The maximum linear model (R package 'stats' version 4.0.5) (RStudio Team, 2021) was tested including all categorical factors (microparticle, virus, and day) and their interactions. The best model was this maximum model, for which a three-way ANOVA was run (R package 'stats' version 4.0.5) (RStudio Team, 2021). Significant differences in three-way interactions between treatments were analyzed with the post-hoc Tukey honest significant differences test (R package 'stats' version 4.0.5) (RStudio Team, 2021), with full comparisons provided in supplementary material and comparisons deemed biologically significant reported.

Genetic markers for immune response were evaluated using linear models (Table S2), and the results of IFNγ and secreted IgT in the gill tissue graphed and analyzed separately. The maximum linear model (R package 'stats' version 4.0.5) included all categorical factors of microparticle, virus, day and their interactions; with ΔCt expression as a response variable. The best linear model was fit to the data and included all factors but not any of their interactions. Although we looked at interactions and did not find them to improve the model, power to resolve

them may have been limited; however, main effects are discussed and their relation to other patterns observed.

Prior to all the analyses, data were analyzed graphically (interquartile and variance plots) to validate normality and homogeneity of variance model assumptions. No outliers were found that justified removal of any data points from the data set. Complete output of statistical analyses and best fit models can be found in the supplementary materials. Results are typically presented with subscripts on test statistic denoting factor, residual degrees of freedom. P-values were rounded to the third decimal place and values less than 0.001 shown as <0.001.

3. Results

3.1 Viral-mediated fish mortality

Fish mortality was monitored daily (Fig. 2). There was no significant mortality (3 of 1560 fish dead) prior to IHNV exposure, regardless of microparticle exposure. The hazard of death increased significantly (354-fold) among fish exposed to virus compared to those unexposed (Cox proportional hazard analysis, $X^2_{1,17.16} = 33.73$, p-value <0.001; Fig. 2). Because virtually no mortality was observed in virus negative treatments, we focused additional analyses on the virus-exposed groups. Among virus-exposed fish, all microparticle types increased mortality compared to no particle exposure treatments; however, the significance and magnitude of this effect depended on particle type and dosage. The greatest increase in mortality was observed in the high dose nylon fiber treatment (10 mg L^{-1}), reaching approximately 80%, compared to 20% for fish with no microparticle exposure, increasing hazard of death by 6.4 times (Fig. 2A; $X^2_{1,15.71} = 11.10$, p-value < 0.001). Despite suggestive trends (i.e., p-value 0.05-0.1), the medium and low nylon fiber dosages (1.0 and 0.1mg L^{-1}) did not significantly increase the hazard of death (p-values >0.05). Exposure to 1 mg L^{-1} polystyrene microplastics increased the hazard of death by

3.2 times ($X^2_{1,15.71} = 4.10$, p-value = 0.043). However, the high and low (10 or 0.1 mg L^{-1}) polystyrene treatments did not have a significant effect. Mortality was not significantly enhanced by co-exposure to spartina microparticles at any concentration (Fig. 2C). The observed temporal kinetics of mortalities was consistent between treatments and with previous *in vivo* IHNV work (Wargo et al., 2010).

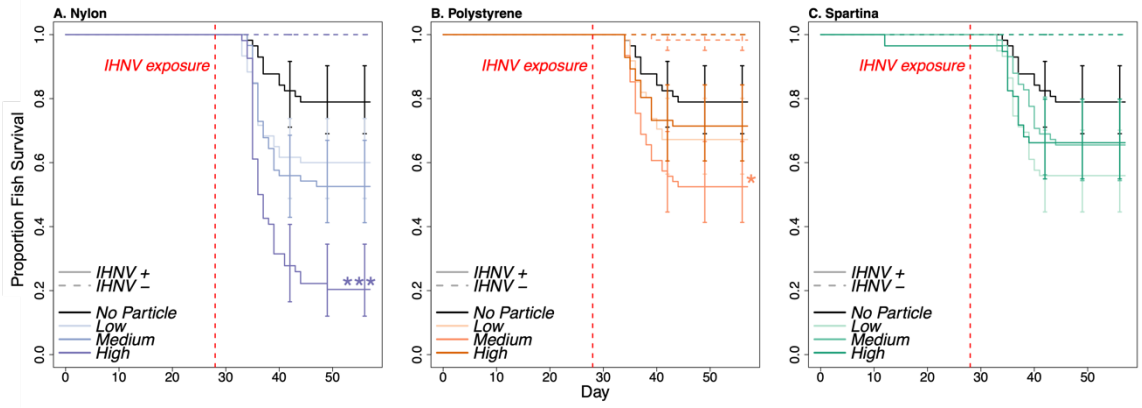

Fig. 2. Co-exposure to IHN virus and microparticles, especially nylon fibers, resulted in increased fish mortalities. Most mortalities occurred between 7 and 17 days following IHNV exposure, illustrated as the proportion of fish surviving over time. Virus unexposed (IHNV-, dashed lines) treatments elicited little to no fish mortality, compared to virus exposed (IHNV+, solid lines). Fish not exposed to any microparticles are denoted with a black line, while microparticle exposures are denoted in blue (nylon, A), orange (polystyrene, B) and green (spartina, C). Color shade corresponds to low (0.1 mg L^{-1}), medium (1.0 mg L^{-1}) and high (10.0 mg L^{-1}) microparticle exposure concentrations. Significant differences in survival between IHNV+ no particle and particle treatments are denoted (Cox proportional hazard analysis, p-value ≤ 0.05 : *, ≤ 0.01 : **, ≤ 0.001 : ***).

316 *3.2 IHNV Shedding and Body Burden*

317 Host entry, replication, and shedding are important factors in understanding viral
318 virulence, fitness, and population level spread (i.e., transmission) (Wargo and Kurath, 2012).
319 Viral shedding in surrounding tank water was quantified at ten different time points following
320 infection (Fig. 3A; all treatment data provided in Fig. S3), providing the total amount of virus
321 shed by all fish in each tank over the previous 24 hours. Previous studies have shown fish to fish
322 variation in shedding can be high, yet the kinetics of viral shed observed here are consistent with
323 traditional single-fish systems (Jones et al., 2020; Wargo et al., 2021), and treatment-level
324 differences were observed. IHNV shedding peaked two to three days post-infection and
325 significantly decreased over time (day effect, linear mixed effects model, $T_{1,229} = -4.9$, p-value <
326 0.001) as fish died (and were removed) or survived and cleared infection. The high nylon dose
327 co-exposed fish shed significantly more virus than fish exposed to virus alone (treatment effect,
328 $T_{1,20} = 2.175$, p-value = 0.042), unlike other microparticle co-exposures. This trend appeared to
329 be primarily driven by the peak period of viral shedding (days 1-4 post exposure to virus) (Figs.
330 2A, S3, S4).
331

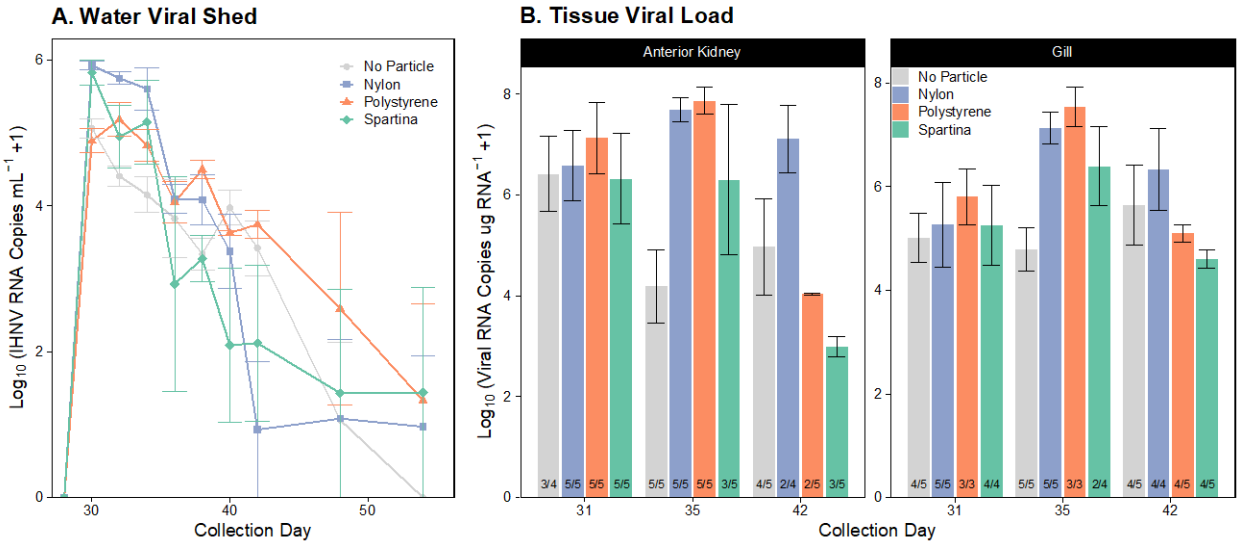

Fig. 3. Viral load in water and tissue samples over time. (A) Virus shed in water is illustrated for the high concentration of each microparticle treatment and no particle control. Points represent mean viral RNA copies uL^{-1} water of triplicate tanks per treatment (±1 standard error of mean (SEM)). Viral shed was significantly influenced by collection day (linear mixed effects model, $T_{1,229} = -4.9$, p-value < 0.001) and higher overall in nylon co-exposed fish than those exposed to virus alone ($T_{1,20} = 2.175$, p-value = 0.042). **(B)** IHNV loads in anterior kidney and gill tissues are presented for each collection day. Bars show mean viral RNA copies in one µg of RNA (±1 SEM) for fish terminally sampled on each day. Only fish with virus detected are included in means; number of virus positive out of total sampled are shown as ratios at the base of each bar.

Host viral tissue burden was quantified in both the anterior kidney and gill at 31, 35 and 42 days (3, 7 and 14 days post-IHNV exposure, respectively; Fig. 3B). The anterior kidney is a key site of IHNV replication and commonly analyzed to quantify IHNV body burden, while the gill is believed to be a primary point of host-entry (Drolet et al., 1994). In the anterior kidney, viral load was significantly influenced by the interaction between microparticle type and

collection day ($F_{6,35}$ = 2.739, p-value = 0.027). In gills, viral load was significantly influenced by nylon microfibers (linear mixed effects model, $T_{1,41}$ = 2.395, p-value = 0.021). Shortly following virus exposure (day 31), viral loads in the anterior kidney and gill of infected fish were similar between microparticle and non-particle treatments. In the anterior kidney, tissue burden was significantly higher in nylon and polystyrene co-exposed fish on day 35, compared to non-particle control (Fig 2, Tukey post-hoc test, p-values = 0.029 and 0.018, respectively). This appears to be driven by an increase in viral load after day 31 for fish exposed to nylon and polystyrene, as well a decrease in viral load for fish not exposed to microparticles, although neither of these trends were significant on their own. No other biologically significant differences were observed between particle types or days in anterior kidney. In the gills, nylon microfiber co-exposure had significantly higher viral loads compared to the no particle IHNV+ treatment, regardless of day ($T_{1,41}$ = 2.395, p-value = 0.021). There was also more virus present in gills on day 35 compared to day 28 across all microparticle types (day main effect, $T_{1,41}$ = 2.284, P=0.028), in this case primarily driven by an increase in particle treatments, with little decrease in no particle treatment, compared to day 31. These trends are similar when fish whose tissue viral loads were below quantitation (i.e., low or no infection) were included (Fig. S5).

3.3 Histopathology

Histopathological analysis was focused on gill tissues as they are an important site of IHNV entry into fish (Drolet et al., 1994). We hypothesized that increased gill pathology associated with microplastic exposure may be a driver of increased mortality in fish. Gill tissues were examined from the same fish for which viral loads were quantified, as well as five terminally sampled fish. Each fish gill was rated on a severity scale from 0 to 3, where 3 was the highest degree of observed tissue response (e.g., respiratory epithelial tissue damage,

372 inflammation, leukocyte invasion; Fig. 4A). In general, gills of fish exposed to IHNV exhibited
373 severe pathology compared to the predominantly normal healthy gill architecture (no particle
374 IHNV-; Fig 3B), significantly so for IHNV+ nylon on days 35, 42 and 56 (post-hoc Tukey's
375 honestly significant difference test p-values <0.001), IHNV+ polystyrene on day 35 (p-value <
376 0.001), and IHNV+ no particle on days 42 and 56 (p-values = 0.024 and 0.017, respectively),
377 within a given day. Spartina/virus co-exposed fish had significantly lower pathology than
378 nylon/virus co-exposed fish on days 35, 42 and 56 (p-values <0.001, 0.024 and 0.024,
379 respectively). In nylon/virus co-exposed fish, pathological severity of IHNV infection was
380 significantly higher in gills sampled on days 35, 42 and 56 than day 31 (p-values <0.001), a sign
381 of worsening infection with time. Likewise, severity of pathology increased significantly from
382 day 31 to 35 for polystyrene co-exposed fish (p-value = 0.002). This rapid increase in severity of
383 tissue pathology compared to the no particle control suggests that microplastic-exposed fish may
384 already have been in a pro-inflammatory state by the time virus challenge was initiated (day 28),
385 or this may be a function of the rapid increase in viral load at this time. It is also possible that the
386 observed increase in pathology over time may have diminished due to rapid mortality of the most
387 susceptible and diseased animals. The suggested plateau or even decrease in pathology on day 56
388 could be evidence of this phenomenon (Fig. 4). Despite such a potential bias, observed
389 pathology was still significantly higher for the nylon/virus treatment, where mortality was the
390 greatest, compared to no particle and spartina particle controls.

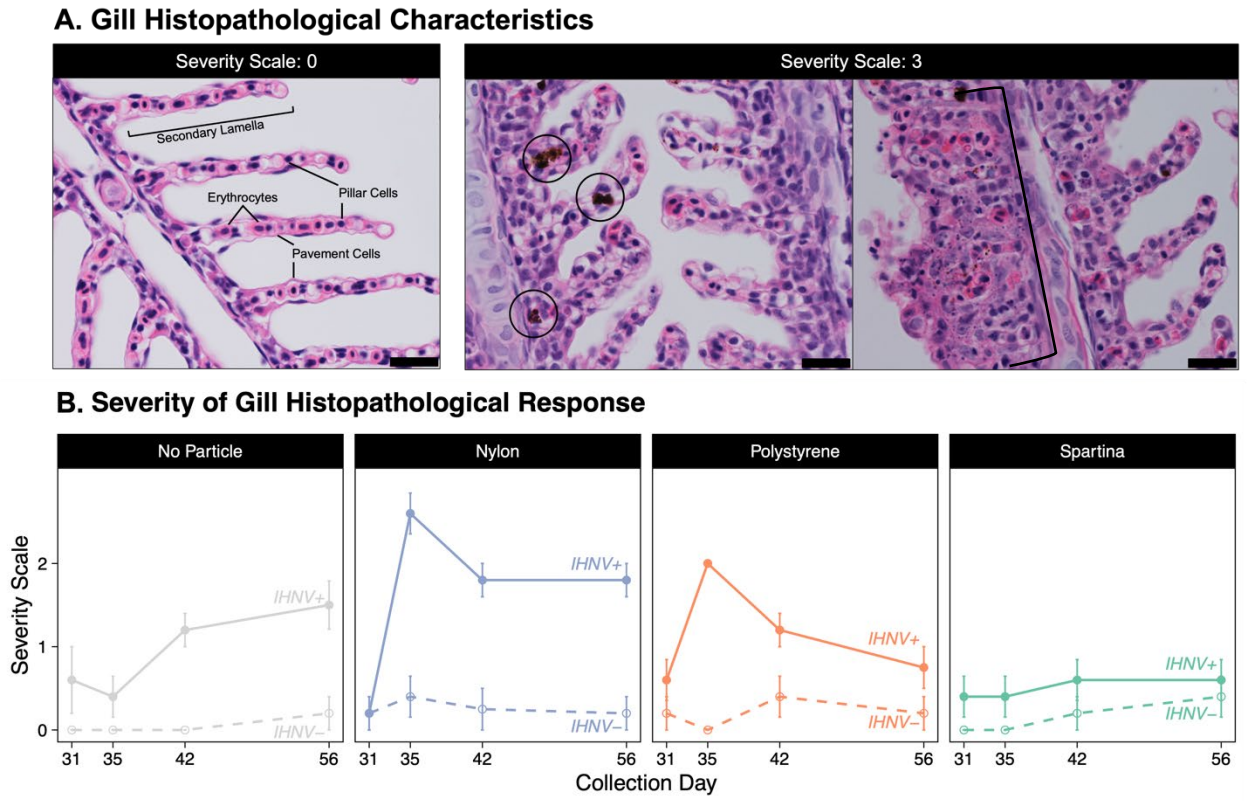

Fig. 4. Histopathological analyses of trout gill tissues. (A) Microscopic images of gill tissues at 40 times magnification (black bar: 20 µm; Olympus AX-70 photomicroscope). Healthy tissue (severity: 0) are on the left and unhealthy tissue sections on the right (severity: 3). Healthy tissue exhibited normal primary gill filament and secondary lamellae cell structure. In contrast, fish with increased pathology exhibited significant damage to the gill tissue, including widespread respiratory epithelial cell hyperpigmentation (prominent areas circled), necrosis (bracketed region in right severity scale 3 image), and inflammation indicated by hypertrophy, hyperplasia and leukocytic infiltrates. **(B)** Pathological severity scale for each particle and virus treatments (IHNV+: solid lines; IHNV-: dashed lines), averaged for each treatment with +/- 1 SEM (n = 5). According to a three-way ANOVA, the severity of histological response was significantly affected by the interaction between microparticle, virus, and collection day ($F_{9,124} = 7.631$, p-value < 0.001).

Evaluation of gill tissues in fish not exposed to IHNV was also essential, as respiration of microplastic-laden water may lead to gill inflammation and pathology. Increased pathology was only observed in a small subset of samples for microparticle-only exposed fish. These exhibited minor sites of focal inflammation, leukocytes infiltration and epithelial damage, recorded as a severity scale of 1 (Fig. 4B; Fig. S6) (Hu et al., 2020). Viral replication may have been enhanced by the low-severity inflammatory response observed in fish exposed to microplastics alone and supports analysis of a pro-inflammatory host response in the gills following microplastic exposure. Moreover, we were unable to identify microplastic particles in histologic tissue sections. This could be due to the multiple rinse steps required for excised gill arch preparation or a lack of substantial microparticle integration into the tissue matrix.

3.4 Immune Response

To further explore gill inflammation and immune response as a cause of increased disease mortality, immune gene expression was evaluated. Several genes spanning the innate and adaptive branches of the immune system were measured in gill and anterior kidney of fish collected for viral load analysis. The relative fold change (RFC) in expression of these genes compared to the day 31 negative control (no particle, IHNV-) was analyzed following standard practices (Livak and Schmittgen, 2001), illustrated for interferon gamma (IFNγ) and secreted immunoglobulin tau (IgT) in gill tissues (Fig. 5). (Other markers' information is provided in supplemental materials and Table S2.)

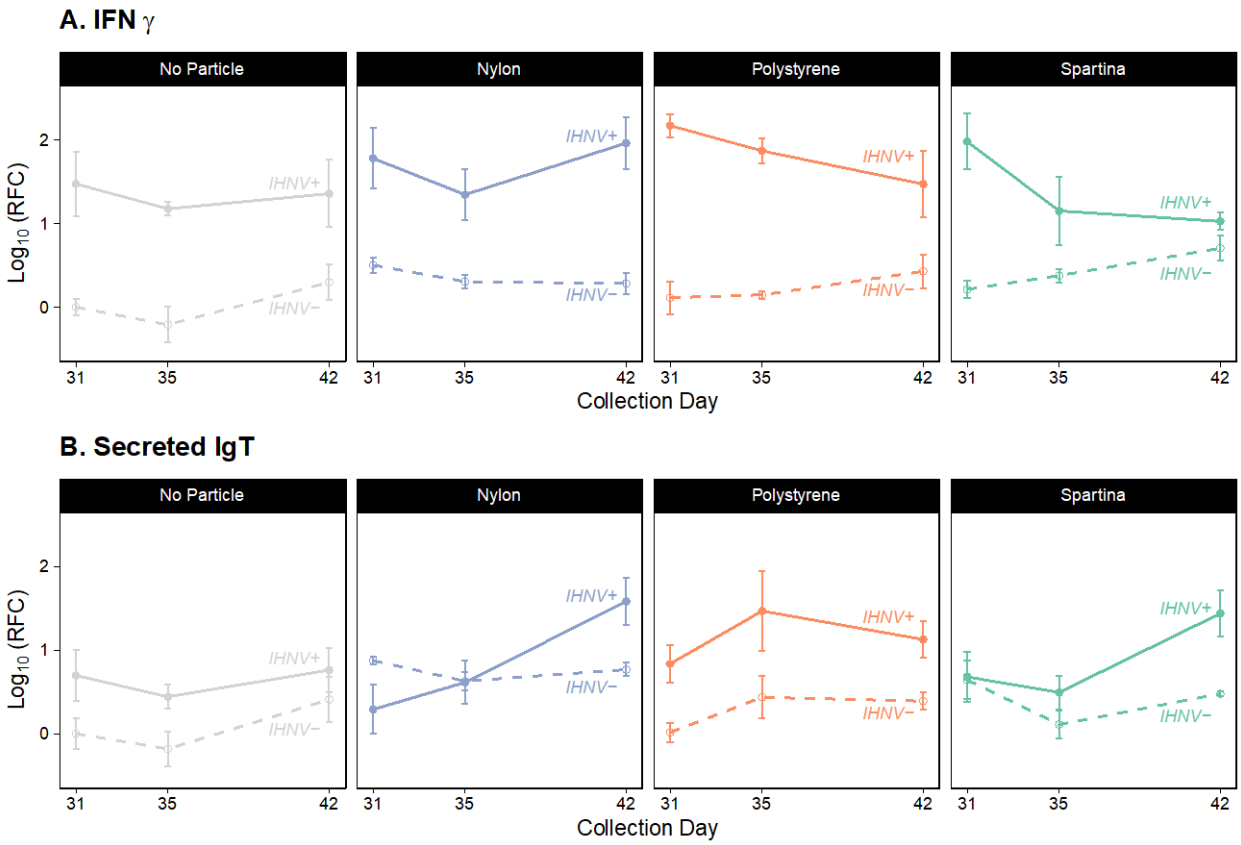

425

426 **Fig. 5. Response of IFNγ (A) and secreted IgT (B) in gill tissue over time.** The relative fold
427 change (RFC; log_{10}-adjusted) compared to the control (no particle, IHNV-) on day 31 is plotted
428 for each microparticle and virus treatment on each collection day, with +/- 1 SEM (n = 5, with
429 exceptions: Table S2). For IFNγ, expression was significantly affected by microparticle, day and
430 virus, but not their interactions (linear mixed effects model, $F_{6,97} = 26.26$, p-value <0.001). For
431 secreted IgT, expression was also significantly affected by microparticle, day and virus, but not
432 their interactions (linear mixed effects model, $F_{6,97} = 7.655$, p-value <0.001).

433

434 IFNγ is integral in early anti-viral activity and commonly analyzed as a marker of IHNV
435 immune response (Purcell et al., 2012, 2010). IFNγ generally triggers pro-inflammatory
436 responses through activation of monocytes and neutrophils (Zou and Secombes, 2016). Previous

437 work has primarily evaluated IFNγ in hematopoietic tissues or whole-body homogenates of
438 juvenile fish, even though gills may be an important site of IHNV entry into host organisms
439 (Dixon et al., 2016; Purcell et al., 2012). We found a marked increase in IFNγ in gills of fish
440 after exposure to virus ($T_{1,97}$=11.92, p-value <0.001), in agreement with previous studies (Purcell
441 et al., 2010). Expression of IFNγ was also significantly higher in fish exposed to nylon
442 microfibers ($T_{1,97}$ = 2.42, p-value = 0.018) and polystyrene microplastics ($T_{1,97}$ = 2.20, p-value =
443 0.03), regardless of virus exposure (Fig. S7). Increased IFNγ expression suggests that
444 microplastics increased the pro-inflammatory state of gills prior to virus exposure. It is likely,
445 therefore, that microplastics acted as a mild physical irritant on the gill respiratory epithelium. To
446 further evaluate innate host defenses beyond IFNγ, we measured expression of macrophage
447 colony stimulating factor receptor (MCSFR) expression, which identifies phagocytic
448 macrophages/monocytes in teleost fishes (Takizawa et al., 2016). No differences in MCSFR
449 expression between treatment groups were observed (Table S2).
450 Secreted IgT is a key component of teleost fish mucosal antibody response (Purcell et al.,
451 2012). Our results demonstrate that infection with IHNV significantly increased secreted IgT
452 expression compared to uninfected fish ($T_{1,97}$ = 4.56, p-value < 0.001), indicating that there was a
453 mucosal antibody response to IHNV in the gills. This response increased over time, as
454 demonstrated by significantly increased expression from day 31 to 42 ($T_{1, 97}$ = 3.01, p-value =
455 0.003). This pattern of initially low and increased expression through time appeared to be most
456 pronounced in the nylon microfiber and IHNV co-exposed fish (and to a lesser degree, spartina
457 microparticle co-exposed fish), suggesting potential delay in secreted IgT response, although
458 there was no statistical interaction between time, microparticle, and/or virus exposure. Secreted
459 IgT expression was significantly higher among fish exposed to nylon, polystyrene or spartina

microparticles ($T_{1,97}$ = 2.81, 2.36, 2.08, and p-values = 0.006, 0.02 and 0.04, respectively) than those not exposed to microparticles, regardless of IHNV exposure (Fig. S8). This suggests that the presence of microparticles increased the mucosal antibody response but that this activation was not protective, as co-exposure to virus and microplastics is correlated with both increased viral load/shedding and mortality in our study. This agrees with other research that has shown correlations between level of inflammation, pathogen load, and disease expression (Quddos and Zwollo, 2021). In addition to secreted IgT, secreted and membrane-bound forms of the more systemic immunoglobulin Mu (IgM) were also analyzed to assess humoral immune response, because *in vitro* work suggested that B-lymphoid development in the anterior kidney was suppressed by the presence of the polystyrene microplastics (Yang, 2020; Zwollo et al., 2021).. We did not observe any change in expression of the membrane form of immunoglobulin mu between treatments in anterior kidney tissues (Table S2). The response was highly variable between sampling times, suggesting our analyses may not have had sufficient temporal resolution or power (limited sample size) to distinguish any relationship between humoral immunity and microparticle exposure *in vivo*. Effects to B-lymphopoeisis sould be most pronounced if microparticles translocated to the tissue of the anterior kidney, but this was not examined in this study.

4. DISCUSSION

Assessment of the risks of microplastic exposure must consider that, in the actual environment, organisms are subject to multiple stressors (e.g., pathogens, toxic chemicals, altered temperature and pH), not just microplastics alone. We hypothesized that microplastics would increase IHNV virulence, while the natural microparticle (spartina) would have no effect

– a product of particle chemistry (natural polymer v. synthetic polymers with chemical additives). Our results were consistent with this hypothesis as only microplastics (nylon microfibers and polystyrene microplastics) had a significant effect on virulence. Toxicity may derive from chemical constituents (Zimmermann et al., 2019), or more simply the higher crystallinity (i.e., hardness) common in synthetic polymers (Andrady, 2017). Expanded polystyrene is commonly used in buoys and floats, as well as single use containers and shipping packaging (Darnerud, 2003; Jang et al., 2017). The polystyrene used here was produced for home insulation and contained the brominated flame retardant hexabromocyclododecane. The nylon microfibers were free of known additives, apart from TiO_2 as a delustrant (manufacturer reported). Spartina is a lignocellulose-based polymer (Hodson et al., 1984). The microparticle treatments with the greatest influence on IHNV virulence (polystyrene and nylon) were composed of petroleum-based polymers, but the expected toxicity of their additives (i.e., hexabromocyclododecane) did not correlate with mortality. This suggests that the physical properties of the microplastics drove effects more than the chemical additive constituents. We note that our experimental design (i.e., tank flushing and dosing every other day) may have diminished possible leachate effect compared to environments where polluted plastic concentrations are chronically high, which is difficult to simulate in a laboratory setting *in vivo*. However, microplastic and leachate concentrations in the environment can be highly variable through time, due to tidal, circulation, or variable inputs (Hale et al., 2020). How this variability influences disease dynamics would be an exciting are of research.

The size and shape of nylon microfibers may also be important drivers of IHNV-induced mortality. Indeed, recent work propounds that microfibers have distinct toxicological impacts (Bucci and Rochman, 2022). Although it is often speculated that smaller particles may have the

506 greatest magnitude of effect due to cellular-level interactions, the polystyrene and spartina in our
507 study were similarly small but enhanced mortality less so than nylon microfibers (Besseling et
508 al., 2019). We calculated (using particle sizes and densities) that our mass-based exposures
509 equated to nearly 100-fold fewer nylon microfibers (approximately 29,000 to 290) than
510 polystyrene microplastics (2,400,000 to 24,000) per liter. This underscores the relative potency
511 of the nylon microfibers; that is, fewer microfibers caused a greater effect than more numerous
512 polystyrene microplastics. By using a large range of doses, we spanned possible environmental
513 concentrations, which are typically stochastic and are likely underestimated due to sampling and
514 analytical biases (Hale et al., 2020).
515 Interestingly, virulence response to nylon microfiber exposure followed a clear dose
516 response, while polystyrene did not. Although dose generally correlates with toxicity, the
517 absence of a dose response in polystyrene-exposed fish may indicate that smaller microparticles
518 (polystyrene and spartina) might have aggregated in water at high doses, effectively decreasing
519 the number of 'particles' to which an organism is exposed. Microplastic agglomeration can be
520 influenced by size, surface charge/chemistry, biofilm formation, microplastic concentration and
521 salinity (Shupe et al., 2021; Summers et al., 2018). We cannot exclude this hypothesis as no
522 mechanisms beyond aeration were used to disperse particles, even though particles were visually
523 observed to disperse within tanks. We do not believe that the lack of a dose response was a result
524 of variation between tanks or individual fish within tanks because this was accounted for in our
525 models by including tank as a random effect (model 1: $X^2_{13.93,17.16} = 34.33$, p-value = 0.002;
526 model 2: $X^2_{13.52,15.71} = 33.82$, p-value = 0.002).
527 The data presented on viral shedding and host viral load support the conclusion that host
528 viral replication increased and, perhaps more importantly, clearance rate decreased when fish

were co-exposed to virus and microplastics (especially nylon microfibers and polystyrene microplastics), leading to exacerbated disease and mortality. This resulted in more viral shedding in the nylon co-exposure. Together, this suggests that the increased mortality associated with exposure to microplastics was driven by higher viral loads for a longer period of time, as well as possibly compromised tolerance for the same viral load. Again, co-exposed microparticle type was an important driver of these dynamics, with nylon having the most pronounced effect. These data agree with previous work that IHNV *in vivo* fitness, particularly duration of infection, can correlate with virulence in fish (Jones et al., 2020; Wargo et al., 2021, 2017, 2010). Further, the increase in shedding following nylon and viral co-exposure suggests that between-host transmission may also be increased by microplastic co-exposure. This has major epidemiological implications for the spread and burden of disease at a population level.

Enhanced in-host and shed viral load among microplastic and virus co-exposed fish was associated with tissue damage . Expression of select markers indicative of host defense mechanisms suggest that microplastic/IHNV co-exposed fish did not exhibit plastic-induced immunosuppression of the marker genes analyzed here. Rather, there was evidence of a pro-inflammatory immune response among uninfected fish exposed to microparticles, particularly microfibers. In addition, although phagocytic cells (including macrophages, monocytes, granulocytic cells, and phagocytic B cells) have been documented to engulf microplastics ≤10 μm *in vitro* (Zwollo et al., 2021), the number of polystyrene or spartina particles of this size encountering fish gills may have been insufficient to trigger a phagocytic response detectable by MCSFR. Neutrophil marker myeloperoxidase (MPO) should be investigated in future work.

One explanation for these results is that microparticles lead to enhanced host viral entry (initially into host barrier epithelial cells) and stress, which lead to reduced viral clearance, when

552 microparticles were present (Fig. 6). Successful host colonization is the first step in establishing
553 infection, to which fish present both physical and immunological defenses (Salinas, 2015; Wargo
554 and Kurath, 2011). Here, microparticles may have damaged epithelia after contact with
555 respiratory surfaces or the digestive tract, if ingested (as demonstrated by Hu et al., 2020) – both
556 sites of IHNV possible host invasion (Bour et al., 2020; Dixon et al., 2016; Hu et al., 2020).
557 Similarly, such tissue damage may cause a proinflammatory or other response in host, and allow
558 for greater IHNV replication or reduced efficacy in virus clearance. The likelihood that a particle
559 could damage associated epithelia and cause stress may be a function of its physical properties.
560 Synthetic polymers may be less flexible (more crystalline) than natural materials (Andrady,
561 2017). Shape may also be critical; asbestos and workers lung are a product of the particle shape,
562 not chemistry (Pimentel et al., 1975; Siegrist and Wylie, 1980). Recent research has found that
563 microplastics can cause intestinal abrasion, and that longer plastic microfibers (≤200 μm) may be
564 more damaging (Zhao et al., 2021). This may explain why smaller polystyrene microplastics
565 enhanced virulence of IHNV (and without a clear dose response), but less so than nylon
566 microfibers, and warrants further investigation. Duration of microparticle exposure prior to
567 pathogen should also be considered; longer exposure times may result in increased tissue damage
568 and inflammation, as seen here, versus shorter exposures without microplastic exposure prior to
569 pathogen introduction (Leads et al., 2019). Further, although microplastic biofilms have been
570 proposed as a viral vector which could enhance exposure pathways (Amaral-Zettler et al., 2020),
571 our fish were actually exposed to IHNV in the absence of microparticles (plastic dosing occurred
572 before and after viral exposure). In a separate *in vitro* study, we observed that viral load was not
573 affected by the presence of microparticles over 48 hours. This indicates that microparticle
574 sorption, leached additives, or unbound monomers did not influence viral exposure

concentrations (Fig. S9). Based on the data gathered here, enhanced host colonization or viral replication caused by physical interactions of the host with microparticles (particularly microfibers) seems a probable explanation, but warrants further investigation.

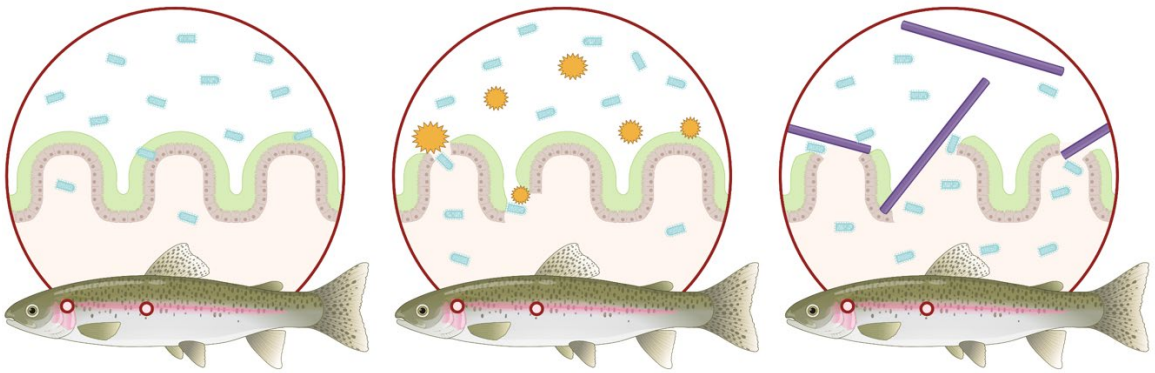

Fig. 6. Proposed mechanism of microplastics increased virulence. When exposed to virus alone (blue virions), mucosal and epithelial barriers of the gill and intestinal tract block some virus from entering the tissues. When exposed to microparticles and then virus, the epithelial/mucosal barrier may incur mild physical damage to membranes causing inflammatory response. Damage is greater for microfibers, which are larger and may be more likely to become entrapped in and damage the outer membrane of delicate epithelia. This may facilitate greater viral entry and host stress (facilitating greater viral replication and reductions in clearance), ultimately increasing disease virulence. Illustration not to scale.

5. Conclusions

Overall, our results demonstrate that exposure to microplastics increased lethality of a serious infectious disease in an economically important fish species. This effect was most pronounced for nylon microfibers. To explore this finding, we evaluated viral shedding, host

viral load, histopathology of the gills and aspects of immune response. We found that fish co-exposed to the highest concentration of nylon microfibers and virus had a greater viral load and shedding, more tissue damage on gills, and pro-inflammatory immune response. Therefore, we hypothesize that the increase lethality of virus in this co-exposure was caused by greater infection severity. Our results have substantial implications, given the widespread distribution and increasing concentrations of microplastics, particularly microfibers. The proposed interactions between microplastics, pathogens and hosts merit further investigation. Importantly, the characteristics of microplastics (i.e., size, shape, chemistry, crystallinity) responsible for eliciting detrimental effects should be explored. The question of whether microparticles of a larger size or microfibers of a natural material cause similar damage also remains open. Our results also indicated microplastic co-exposure may enhance viral transmission. This could have major epidemiological consequences, such as increase pathogen prevalence and spillover from plastic-exposed to non-exposed populations. Our findings have implications across a range of aquatic and terrestrial host-pathogen systems. This includes humans, who are also coincidentally exposed to microplastics and infectious agents in indoor environments (Prata et al., 2020); the latter has been dramatically illustrated in the case of the SARS-CoV-2 virus (Chen et al., 2021). Host and pathogen systems such as the one used here can serve as a model for the relationship between pathogens and microplastics, and interdisciplinary work regarding the mechanisms underlying this relationship should be prioritized. This study supports the supposition that microplastics may be a global threat, of which the ramifications must be considered in the context of multiple stressors and realistic ecosystems.

Acknowledgements

We immensely appreciate support from: Barbara Rutan with experimental and analytical setup; Tim Leeds and Greg Wiens from the NCCCWA USDA lab for supplying fish; Hannah Brown with fish care and experimental setup; Malina Loeher with evaluation of virus sorption to particles and experimental setup; Drew Luellen with contributing microplastics for exposure and additive analysis; Lidia Epp with molecular analyses; Melanie Kolacy with tissue preparation and embedding; and Jennifer Connell with particle size analysis. Abstract art and Figure 5 were created with biorender.com.

Funding

National Oceanic and Atmospheric Administration Marine Debris Program (Award #: NA19NOS9990085). Support for M. E. Seeley was generously provided by the Freeman Family Foundation.

CRediT authorship contribution statement

MES contributed to conceptualization, methodology, formal analysis, investigation, data curation, writing – original draft, writing – review & editing, visualization, project administration, funding acquisition. RCH contributed to conceptualization, methodology, resources, writing – review & editing, supervision, project administration, funding acquisition. PXZ contributed to conceptualization, methodology, resources, writing – review & editing, visualization, project administration, funding acquisition. WKV contributed to conceptualization, methodology, resources, writing – review & editing, visualization, project administration, funding acquisition. GV contributed to investigation and data curation. ARW contributed to conceptualization, methodology, formal analysis, resources, writing – review & editing, supervision, project administration, funding acquisition.

References

Amaral-Zettler, L.A., Zettler, E.R., Mincer, T.J., 2020. Ecology of the plastisphere. Nat. Rev. Microbiol. 18, 139–151. https://doi.org/10.1038/s41579-019-0308-0

Andrady, A.L., 2017. The plastic in microplastics: A review. Mar. Pollut. Bull. 119, 12–22. https://doi.org/10.1016/j.marpolbul.2017.01.082

Athey, S.N., Erdle, L.M., 2021. Are We Underestimating Anthropogenic Microfiber Pollution? A Critical Review of Occurrence, Methods, and Reporting. Environ. Toxicol. Chem. 41, 822–837. https://doi.org/10.1002/etc.5173

Besseling, E., Redondo-Hasselerharm, P., Foekema, E.M., Koelmans, A.A., 2019. Quantifying ecological risks of aquatic micro- and nanoplastic. Crit. Rev. Environ. Sci. Technol. 49, 32–80. https://doi.org/10.1080/10643389.2018.1531688

Bootland, L., Leong, J.-A., 2011. Infectious haematopoietic necrosis virus, in: Fish Diseases and Disorders. pp. 66–109.

Borrelle, S.B., Ringma, J., Law, K.L., Monnahan, C.C., Lebreton, L., McGivern, A., Murphy, E., Jambeck, J., Leonard, G.H., Hilleary, M.A., Eriksen, M., Possingham, H.P., De Frond, H., Gerber, L.R., Polidoro, B., Tahir, A., Bernard, M., Mallos, N., Barnes, M., Rochman, C.M., 2020. Predicted growth in plastic waste exceeds efforts to mitigate plastic pollution. Science 369, 1515–1518. https://doi.org/10.1126/science.aba3656

Bour, A., Hossain, S., Taylor, M., Sumner, M., Carney Almroth, B., 2020. Synthetic Microfiber and Microbead Exposure and Retention Time in Model Aquatic Species Under Different Exposure Scenarios. Front. Environ. Sci. 8, 83. https://doi.org/10.3389/fenvs.2020.00083

Bucci, K., Rochman, C.M., 2022. Microplastics: a multidimensional contaminant requires a multidimensional framework for assessing risk. Microplastics Nanoplastics 2, 7. https://doi.org/10.1186/s43591-022-00028-0

Bucci, K., Tulio, M., Rochman, C.M., 2020. What is known and unknown about the effects of plastic pollution: A meta-analysis and systematic review. Ecol. Appl. 30, e02044. https://doi.org/10.1002/eap.2044

Chen, B., Jia, P., Han, J., 2021. Role of indoor aerosols for COVID-19 viral transmission: a review. Environ. Chem. Lett. 19, 1953–1970. https://doi.org/10.1007/s10311-020-01174-8

Darnerud, P.O., 2003. Toxic effects of brominated flame retardants in man and in wildlife. Environ. Int. 29, 841–853. https://doi.org/10.1016/S0160-4120(03)00107-7

Dixon, P., Paley, R., Alegria-Moran, R., Oidtmann, B., 2016. Epidemiological characteristics of infectious hematopoietic necrosis virus (IHNV): a review. Vet. Res. 47, 63. https://doi.org/10.1186/s13567-016-0341-1

Drolet, B.S., Rohovec, J.S., Leong, J.C., 1994. The route of entry and progression of infectious haematopoietic necrosis virus in Oncorhynchus mykiss (Walbaum): a sequential immunohistochemical study. J. Fish Dis. 17, 337–344. https://doi.org/10.1111/j.1365-2761.1994.tb00229.x

Everson, J.L., Jones, D.R., Taylor, A.K., Rutan, B.J., Leeds, T.D., Langwig, K.E., Wargo, A.R., Wiens, G.D., 2021. Aquaculture Reuse Water, Genetic Line, and Vaccination Affect Rainbow Trout (Oncorhynchus mykiss) Disease Susceptibility and Infection Dynamics. Front. Immunol. 12, 3894. https://doi.org/10.3389/fimmu.2021.721048

Gauthier, D., Haines, A., Vogelbein, W., 2021. Elevated temperature inhibits Mycobacterium shottsii infection and Mycobacterium pseudoshottsii disease in striped bass Morone saxatilis. Dis. Aquat. Organ. 144, 159–174. https://doi.org/10.3354/dao03584

Geyer, R., Jambeck, J.R., Law, K.L., 2017. Production, use, and fate of all plastics ever made. Sci. Adv. 3, e1700782. https://doi.org/10.1126/sciadv.1700782

Hale, R.C., Seeley, M.E., La Guardia, M.J., Mai, L., Zeng, E.Y., 2020. A Global Perspective on Microplastics. J. Geophys. Res. Oceans 125, e2018JC014719. https://doi.org/10.1029/2018JC014719

Hodson, R., Christian, R., Maccubbin, A., 1984. Lignocellulose and lignin in the salt marsh grass Spartina alterniflora: initial concentrations and short-term, post-depositional changes in detrital matter 81, 1–7. https://doi.org/10.1007/BF00397619

Hu, L., Chernick, M., Lewis, A.M., Ferguson, P.L., Hinton, D.E., 2020. Chronic microfiber exposure in adult Japanese medaka (Oryzias latipes). PLOS ONE 15, e0229962. https://doi.org/10.1371/journal.pone.0229962

Jang, M., Shim, W.J., Han, G.M., Rani, M., Song, Y.K., Hong, S.H., 2017. Widespread detection of a brominated flame retardant, hexabromocyclododecane, in expanded polystyrene marine debris and microplastics from South Korea and the Asia-Pacific coastal region. Environ. Pollut. 231, 785–794. https://doi.org/10.1016/j.envpol.2017.08.066

Jennings, S., Stentiford, G.D., Leocadio, A.M., Jeffery, K.R., Metcalfe, J.D., Katsiadaki, I., Auchterlonie, N.A., Mangi, S.C., Pinnegar, J.K., Ellis, T., Peeler, E.J., Luisetti, T., Baker-Austin, C., Brown, M., Catchpole, T.L., Clyne, F.J., Dye, S.R., Edmonds, N.J., Hyder, K., Lee, J., Lees, D.N., Morgan, O.C., O'Brien, C.M., Oidtmann, B., Posen, P.E., Santos, A.R., Taylor, N.G.H., Turner, A.D., Townhill, B.L., Verner-Jeffreys, D.W., 2016. Aquatic food security: insights into challenges and solutions from an analysis of interactions between fisheries, aquaculture, food safety, human health, fish and human welfare, economy and environment. Fish Fish. 17, 893–938. https://doi.org/10.1111/faf.12152

Jones, D.R., Rutan, B.J., Wargo, A.R., 2020. Impact of Vaccination and Pathogen Exposure Dosage on Shedding Kinetics of Infectious Hematopoietic Necrosis Virus (IHNV) in Rainbow Trout. J. Aquat. Anim. Health 32, 95–108. https://doi.org/10.1002/aah.10108

Lamb, J.B., Willis, B.L., Fiorenza, E.A., Couch, C.S., Howard, R., Rader, D.N., True, J.D., Kelly, L.A., Ahmad, A., Jompa, J., Harvell, C.D., 2018. Plastic waste associated with disease on coral reefs. Science 359, 460–462. https://doi.org/10.1126/science.aar3320

Leads, R.R., Burnett, K.G., Weinstein, J.E., 2019. The Effect of Microplastic Ingestion on Survival of the Grass Shrimp *Palaemonetes pugio* (Holthuis, 1949) Challenged with *Vibrio campbellii*. Environ. Toxicol. Chem. 38, 2233–2242. https://doi.org/10.1002/etc.4545

Leslie, H.A., J. M. van Velzen, M., Brandsma, S.H., Vethaak, D., Garcia-Vallejo, J.J., Lamoree, M.H., 2022. Discovery and quantification of plastic particle pollution in human blood. Environ. Int. 163, 107199. https://doi.org/10.1016/j.envint.2022.107199

Livak, K.J., Schmittgen, T.D., 2001. Analysis of Relative Gene Expression Data Using Real-Time Quantitative PCR and the 2−ΔΔCT Method. Methods 25, 402–408. https://doi.org/10.1006/meth.2001.1262

MacLeod, M., Arp, H.P.H., Tekman, M.B., Jahnke, A., 2021. The global threat from plastic pollution. Science 373, 61–65. https://doi.org/10.1126/science.abg5433

727 Pimentel, J.C., Avila, R., Lourenço, A.G., 1975. Respiratory disease caused by synthetic fibres: a
728 new occupational disease. Thorax 30, 204–219.
729 Pinheiro, J., Bates, D., DebRoy, S., Sakar, D., 2021. _nlme: Linear and Nonlinear Mixed Effects
730 Models_. R package version 3.1-152.
731 Prata, J.C., da Costa, J.P., Lopes, I., Duarte, A.C., Rocha-Santos, T., 2020. Environmental
732 exposure to microplastics: An overview on possible human health effects. Sci. Total
733 Environ. 702, 134455. https://doi.org/10.1016/j.scitotenv.2019.134455
734 Purcell, M., Thompson, R., Garver, K., Hawley, L., Batts, W., Sprague, L., Sampson, C.,
735 Winton, J., 2013. Universal reverse-transcriptase real-time PCR for infectious
736 hematopoietic necrosis virus (IHNV). Dis. Aquat. Organ. 106, 103–115.
737 https://doi.org/10.3354/dao02644
738 Purcell, M.K., Laing, K.J., Winton, J.R., 2012. Immunity to Fish Rhabdoviruses. Viruses 4, 140–
739 166. https://doi.org/10.3390/v4010140
740 Purcell, M.K., LaPatra, S.E., Woodson, J.C., Kurath, G., Winton, J.R., 2010. Early viral
741 replication and induced or constitutive immunity in rainbow trout families with
742 differential resistance to Infectious hematopoietic necrosis virus (IHNV). Fish Shellfish
743 Immunol. 28, 98–105. https://doi.org/10.1016/j.fsi.2009.10.005
744 Quddos, F., Zwollo, P., 2021. A BCWD-Resistant line of rainbow trout is less sensitive to
745 cortisol implant-induced changes in IgM response as compared to a susceptible (control)
746 line. Dev. Comp. Immunol. 116, 103921. https://doi.org/10.1016/j.dci.2020.103921
747 Ragusa, A., Svelato, A., Santacroce, C., Catalano, P., Notarstefano, V., Carnevali, O., Papa, F.,
748 Rongioletti, M.C.A., Baiocco, F., Draghi, S., D'Amore, E., Rinaldo, D., Matta, M.,
749 Giorgini, E., 2021. Plasticenta: First evidence of microplastics in human placenta.
750 Environ. Int. 146, 106274. https://doi.org/10.1016/j.envint.2020.106274
751 Rochman, C.M., Brookson, C., Bikker, J., Djuric, N., Earn, A., Bucci, K., Athey, S., Huntington,
752 A., McIlwraith, H., Munno, K., De Frond, H., Kolomijeca, A., Erdle, L., Grbic, J.,
753 Bayoumi, M., Borrelle, S.B., Wu, T., Santoro, S., Werbowski, L.M., Zhu, X., Giles, R.K.,
754 Hamilton, B.M., Thaysen, C., Kaura, A., Klasios, N., Ead, L., Kim, J., Sherlock, C., Ho,
755 A., Hung, C., 2019. Rethinking microplastics as a diverse contaminant suite. Environ.
756 Toxicol. Chem. 38, 703–711. https://doi.org/10.1002/etc.4371
757 RStudio Team, 2021. _RStudio: Integrated Development Environment for R_.
758 Salinas, I., 2015. The Mucosal Immune System of Teleost Fish. Biology 4, 525–539.
759 https://doi.org/10.3390/biology4030525
760 Seeley, M.E., Song, B., Passie, R., Hale, R.C., 2020. Microplastics affect sedimentary microbial
761 communities and nitrogen cycling. Nat. Commun. 11, 2372.
762 https://doi.org/10.1038/s41467-020-16235-3
763 Shupe, H.J., Boenisch, K.M., Harper, B.J., Brander, S.M., Harper, S.L., 2021. Effect of
764 Nanoplastic Type and Surface Chemistry on Particle Agglomeration over a Salinity
765 Gradient. Environ. Toxicol. Chem. 40, 1820–1826. https://doi.org/10.1002/etc.5030
766 Siegrist, H.G., Wylie, A.G., 1980. Characterizing and discriminating the shape of asbestos
767 particles. Environ. Res. 23, 348–361.
768 Springman, K.R., Kurath, G., Anderson, J.J., Emlen, J.M., 2005. Contaminants as viral cofactors:
769 assessing indirect population effects. Aquat. Toxicol. 71, 13–23.
770 https://doi.org/10.1016/j.aquatox.2004.10.006

Summers, S., Henry, T., Gutierrez, T., 2018. Agglomeration of nano- and microplastic particles in seawater by autochthonous and de novo-produced sources of exopolymeric substances. Mar. Pollut. Bull. 130, 258–267. https://doi.org/10.1016/j.marpolbul.2018.03.039

Takizawa, F., Magadan, S., Parra, D., Xu, Z., Korytář, T., Boudinot, P., Sunyer, J.O., 2016. Novel Teleost CD4-Bearing Cell Populations Provide Insights into the Evolutionary Origins and Primordial Roles of CD4+ Lymphocytes and CD4+ Macrophages. J. Immunol. 196, 4522–4535. https://doi.org/10.4049/jimmunol.1600222

Therneau, T., 2015. A package for survival analysis in S, version 2.38.

Wargo, A.R., Garver, K.A., Kurath, G., 2010. Virulence correlates with fitness in vivo for two M group genotypes of Infectious hematopoietic necrosis virus (IHNV). Virology 404, 51–58. https://doi.org/10.1016/j.virol.2010.04.023

Wargo, A.R., Kurath, G., 2012. Viral fitness: definitions, measurement, and current insights. Curr. Opin. Virol. 2, 538–545. https://doi.org/10.1016/j.coviro.2012.07.007

Wargo, A.R., Kurath, G., 2011. In Vivo Fitness Associated with High Virulence in a Vertebrate Virus Is a Complex Trait Regulated by Host Entry, Replication, and Shedding. J. Virol. 85, 3959–3967. https://doi.org/10.1128/JVI.01891-10

Wargo, A.R., Kurath, G., Scott, R.J., Kerr, B., 2021. Virus shedding kinetics and unconventional virulence tradeoffs. PLOS Pathog. 17, e1009528. https://doi.org/10.1371/journal.ppat.1009528

Wargo, A.R., Scott, R.J., Kerr, B., Kurath, G., 2017. Replication and shedding kinetics of infectious hematopoietic necrosis virus in juvenile rainbow trout. Virus Res. 227, 200–211. https://doi.org/10.1016/j.virusres.2016.10.011

Yang, H., 2020. Polystyrene microplastics decrease F-53B bioaccumulation but induce inflammatory stress in larval zebrafish. Chemosphere 8. https://doi.org/10.1016/j.chemosphere.2020.127040

Zhao, Y., Qiao, R., Zhang, S., Wang, G., 2021. Metabolomic profiling reveals the intestinal toxicity of different length of microplastic fibers on zebrafish (Danio rerio). J. Hazard. Mater. 403, 123663. https://doi.org/10.1016/j.jhazmat.2020.123663

Zimmermann, L., Dierkes, G., Ternes, T.A., Völker, C., Wagner, M., 2019. Benchmarking the in Vitro Toxicity and Chemical Composition of Plastic Consumer Products. Environ. Sci. Technol. 53, 11467–11477. https://doi.org/10.1021/acs.est.9b02293

Zou, J., Secombes, C., 2016. The Function of Fish Cytokines. Biology 5, 23. https://doi.org/10.3390/biology5020023

Zwollo, P., Quddos, F., Bagdassarian, C., Seeley, M.E., Hale, R.C., Abderhalden, L., 2021. Polystyrene microplastics reduce abundance of developing B cells in rainbow trout (Oncorhynchus mykiss) primary cultures. Fish Shellfish Immunol. 114, 102–111. https://doi.org/10.1016/j.fsi.2021.04.014